J. Membrane Biol. 128, 123–132 (1992)

The Journal of
Membrane Biology


# Transient Outwardly Rectifying Potassium Channel in the Rabbit Corneal Endothelium

Mitchell A. Watsky, Kim Cooper, and James L. Rae
Departments of Physiology and Biophysics and Ophthalmology, Mayo Foundation Rochester, Minnesota 55905

**Summary.** Ionic currents from freshly dissociated rabbit corneal endothelial cells were examined using patch-clamp technology and a perforated patch technique. Whole-cell current recordings revealed a transient outward $K^+$-selective current that was blockable in a dose-dependent manner by 4-aminopyridine (4-AP) and quinidine. This current is similar to the '*A*'-type current present in many excitable cells and is the first reported instance of such a current in any epithelial cell type. In addition to the transient current, an outwardly rectifying nonselective cation current was also observed. This current is also blocked by quinidine.

To examine the possible role of these currents in the stromal volume regulatory function of the endothelium, corneas were perfused under a specular microscope with a glutathione-bicarbonate Ringer's solution (GBR) or GBR plus either 1 mM quinidine or 10 mM 4-AP. For quinidine perfusions, control corneas swelled at a rate of 6 $\mu$m/hr, while quinidine-perfused corneas swelled at a rate of 48 $\mu$m/hr. For 4-AP perfusions, control corneas deswelled at a rate of $-2$ $\mu$m/hr, while 4-AP perfused corneas swelled at a rate of 24 $\mu$m/hr. One possible mechanism of the stromal swelling induced by these $K^+$ channel blockers may be the result of loss of the $K^+$ recycling pathway necessary for proper $Na^+/K^+$ ATPase function.

**Key Words** cornea · *A*-type potassium channel · epithelium · patch clamp · perforated patch

## Introduction

The corneal endothelium is the primary regulator of corneal hydration. Although it is well known that the $Na^+/K^+$ ATPase plays a significant role in the fluid-moving mechanism of these cells, the cycling and recycling pathways for $Na^+$ and $K^+$ movement outside of this transporter have not been completely characterized. To date, four channel types have been described in the corneal endothelium (two in detail), three by single channel patch-clamp analysis. The first channel described is a frequently occurring, highly selective $K^+$ channel. This channel is activated by external anions, as well as the stilbene derivative, DIDS, and is blocked by $Cs^+$ (Rae, Dewey & Cooper, 1989). The second well-characterized channel is a nonselective cation channel that is activated by internal calcium and inhibited by internal ATP (Rae et al., 1990). Quinidine, when applied to the cytoplasmic surface, produces a flickery block of the channel. A third channel type, described only briefly, is a large conductance anion channel (Rae, Levis & Eisenberg, 1988). Lastly, a voltage-sensitive $Na^+$ channel that is blockade by tetrodotoxin and quinidine has been described using whole cell techniques (Watsky, Cooper & Rae, 1991).

The purpose of the present study was to record whole-cell currents from the corneal endothelium, to characterize the major conductance pathways, and to determine if the channels associated with these conductive pathways contribute to the corneal deturgescence function of the endothelium. Surprisingly, one of the predominant currents observed was a voltage-sensitive, transient $K^+$ current with properties very similar to the '*A*'-type channel seen previously only in excitable cells. To the best of our knowledge, this is the first description of an *A*-type $K^+$ channel in any epithelial cell type. In vitro perfusion of the corneal endothelium with blockers of this channel type induces corneal swelling, indicating a possible physiological role for the channels in maintaining corneal hydration. Along with this *A*-type channel, the other predominant current appears to be a nonselective cation channel that is *not* inhibited by internal ATP.

## Materials and Methods

### Patch-Clamp Studies

All experiments were performed on freshly dissociated corneal endothelial cells from 2–3 kg New Zealand white rabbits. Cells were dissociated in Enzyme Free Dissociation Solution (Specialty Media, Lavallette, NJ) using techniques described previously (Watsky & Rae, 1991; Watsky et al., 1991). Most cells

**Table 1.**

| Solution# | 1 | 2 | 3 | 4 | 5 | 6 | 7 | GBR |
|---|---|---|---|---|---|---|---|---|
| NaCl | — | 15 | 149.2 | — | — | — | — | 111.6 |
| KCl | 27 | — | 4.7 | 150 | — | — | — | 0.4 |
| $KMeSO_4$ | 120 | 130 | — | — | — | — | — | — |
| $CaCl_2$ | 2.5 | 1.0 | 2.5 | 2.5 | 2.5 | 2.5 | 2.5 | 1.04 |
| $MgCl_2$ | — | 1.5 | — | — | — | — | — | 0.9 |
| $NaH_2PO_4$ | — | — | — | — | — | — | — | 0.9 |
| $NaHCO_3$ | — | — | — | — | — | — | — | 29.2 |
| RbCl | — | — | — | — | 150 | — | — | — |
| CsCl | — | — | — | — | — | 150 | — | — |
| LiCl | — | — | — | — | — | — | 150 | — |
| $Na_2ATP$ | — | 5 | — | — | — | — | — | — |
| Glucose | — | 5 | 5 | 5 | — | — | — | 5 |
| Glutathione | — | — | — | — | — | — | — | 0.3 |
| HEPES | 5 | 5 | 5 | 5 | 5 | 5 | 5 | — |
| EGTA | — | 3 | — | — | — | — | — | — |
| OSM | 284 | 300 | 288 | 293 | 292 | 287 | 307 | 285 |
| pH | 7.0 | 7.35 | 7.35 | 7.35 | 7.35 | 7.35 | 7.35 | 7.4 |

were patch clamped using the perforated patch technique, with amphotericin B (Sigma #A-4888), as the permeabilizing agent. This technique has been described in detail previously (Rae et al., 1991; Watsky et al., 1991; Watsky & Rae, 1991). Electrodes were constructed from Corning 7052 and Kimble KG-12 glasses.

Experiments designed to test the effects of internal ATP on the whole-cell currents were carried out using the traditional whole-cell technique as described previously for corneal endothelial cells (Watsky & Rae, 1991), and only Corning 7052 electrodes were used. A listing of solutions is provided in Table 1. All patch-clamp experiments were done at room temperature. Experiments were performed using an Axopatch 1-D patch clamp. Pulse protocols were generated using pClamp software (Axon Instruments, Foster City, CA) running on a modified IBM AT computer. The current records were filtered through a 4-pole Bessel filter at a bandwidth of 1–2 kHz and digitized at a sample rate of 200–400 $\mu$sec/point using an Axolab 12-bit analog to digital converter. Recordings were capacity compensated using the patch-clamp circuitry.

### Perfusion Studies

Corneal perfusions were performed using the procedure of Dikstein and Maurice (1972). Briefly, 2–3 kg New Zealand White rabbits were killed with an overdose of pentobarbital, and their eyes were immediately enucleated. The corneas were then carefully dissected from the globe along with a scleral rim, and clamped endothelial side down along the scleral rim onto two acrylic plastic blocks. The blocks contained inflow and outflow ports to which 20 cc syringes and outflow collectors (respectively) were attached. Corneas were perfused with a glutathione-bicarbonate Ringer's solution (*see* Table 1) at 20 $\mu$l/min using a Harvard Apparatus perfusion pump. Perfusion pressure was maintained at approximately 18 mm Hg by elevating the outflow container to 24.5 cm above the outflow port. The corneas were placed in water jacketed, temperature controlled chambers and maintained at 37°C. The chambers were attached to a specular microscope with a calibrated fine focus adjustment, which was used to make corneal thickness measurements. Silicone oil was applied to the epithelial surface to prevent evaporation from the stroma. Corneal thickness measurements were taken every 15 min by focusing from the epithelial surface down to the endothelial surface, while noting the thickness values on the fine focus knob. Thickness calibration was carried out on silicone oil immersed glass plates of known thickness.

Paired corneas were perfused with control solution (GBR) for one hour to allow for thickness stabilization, after which time the cornea showing the least amount of swelling was perfused with the experimental solution. Thickness readings continued every 15 min up to 3 hr. Analysis of the data was performed by averaging the change in thicknesses from the time point just prior to the solution change. These values were then fit with a linear regression, and the slope was taken to be the swelling rate.

All animals were housed in an NIH-approved facility, and all studies adhered to the ARVO resolution concerning the use of animals in eye research.

## Results

### Patch-Clamp Studies

Freshly dissociated endothelial cells were similar in size, with an average capacitance (± SE) of 6.60 ± 0.39 pF ($n$ = 149). The cells had an average input resistance of 9.8 ± 0.5 GΩ (mean ± SE; $n$ = 26) as measured at the resting potential of the individual cells. Figure 1 illustrates the typical currents seen during perforated patch experiments using a normal Ringer's solution in the bath (Solution 3, Table 1) and a $KMeSO_4$ solution in the electrode (Solution 1). Cells were held at a resting potential of −60 mV, with 16 +10-mV steps then being applied from a starting voltage of −80 mV. Cells were returned to the −60 mV holding voltage at the end of each de-

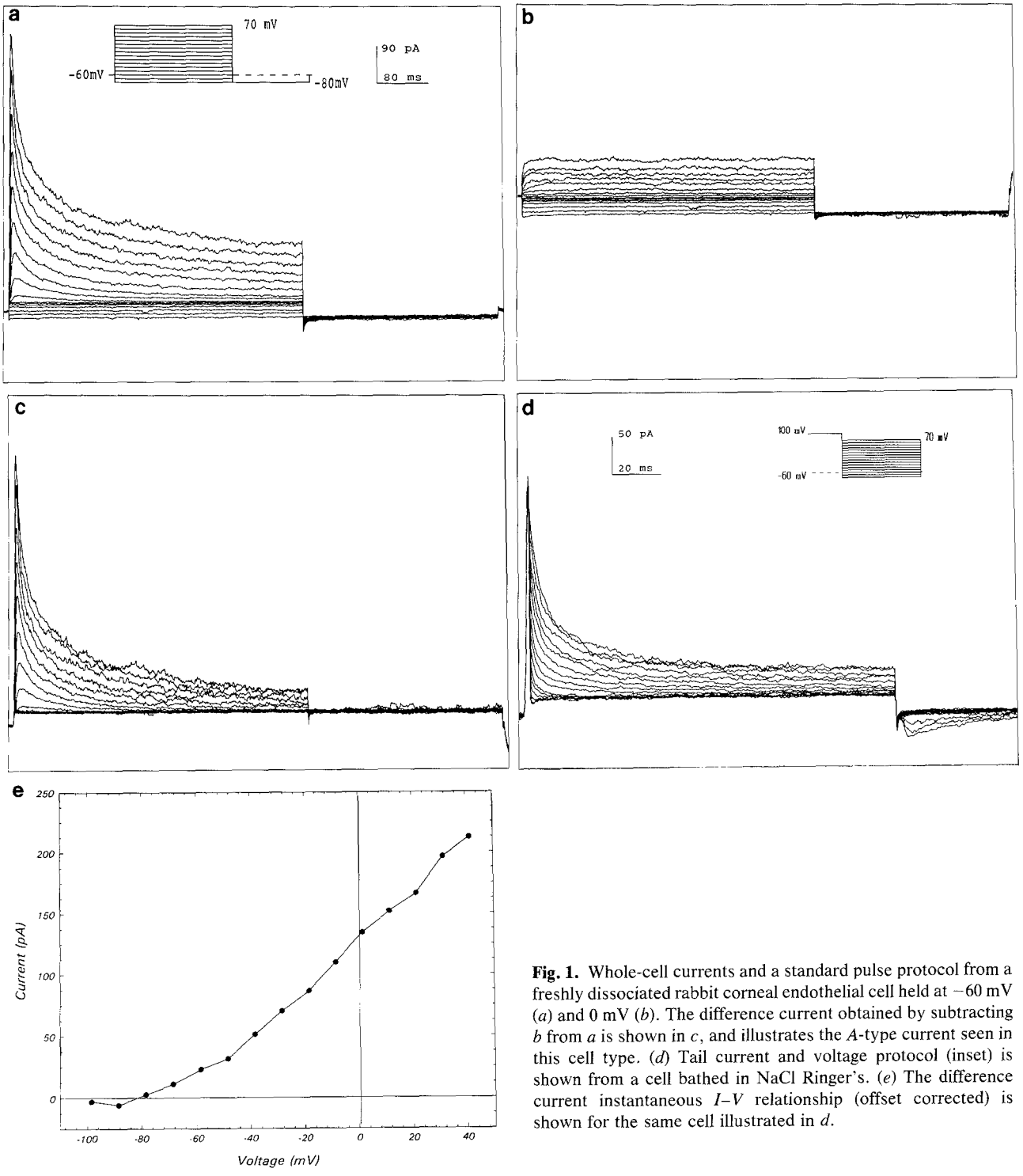


**Fig. 1.** Whole-cell currents and a standard pulse protocol from a freshly dissociated rabbit corneal endothelial cell held at −60 mV (*a*) and 0 mV (*b*). The difference current obtained by subtracting *b* from *a* is shown in *c*, and illustrates the *A*-type current seen in this cell type. (*d*) Tail current and voltage protocol (inset) is shown from a cell bathed in NaCl Ringer's. (*e*) The difference current instantaneous *I–V* relationship (offset corrected) is shown for the same cell illustrated in *d*.

polarizing step (Fig. 1*a*, inset). An identical protocol was also carried out using a holding potential of 0 mV, which completely inactivated the 'A'-type current (Fig. 1*b*). To obtain "uncontaminated" records of the 'A'-type current, the current traces from the 0 mV holding potential experiments were subtracted from those of the −60 mV holding potential experiments for all voltages tested (these will be referred to as the difference currents; Fig. 1*c*). For records that still contained a noninactivating (or very long inactivation time constant) current, the current flowing through the *A*-type channels will be

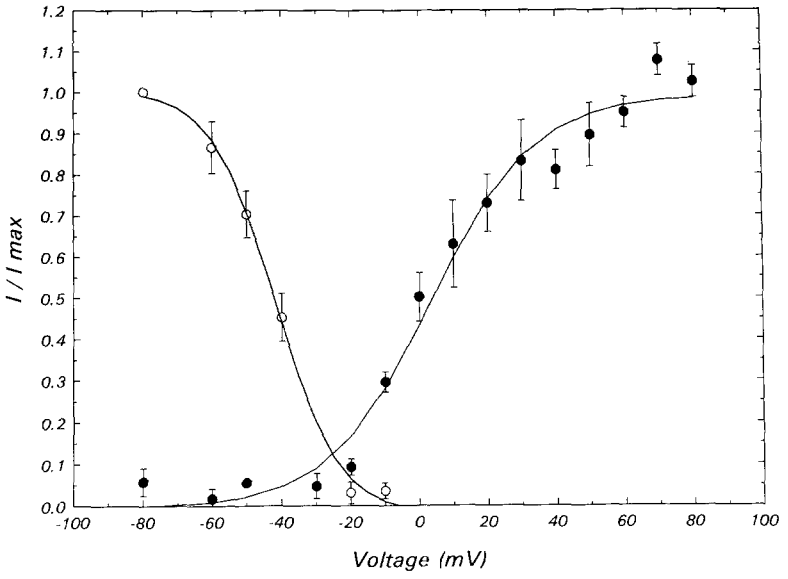


**Fig. 2.** Voltage dependence of steady-state activation (filled circles) and inactivation (open circles) open probabilities (mean ± SE). Activation was determined using a tail current protocol that utilized incremented depolarizing steps followed by a hyperpolarization to the same voltage (−80 mV) ($n$ = 3). Inactivation points were obtained using the protocol described in Fig. 1 with several different holding potentials ($n$ = 4). Difference currents were used in all cases, and open probabilities were determined by dividing $I/I_{max}$. Curves represent the fit to a Boltzmann distribution.

**Table 2.**

| | Corneal endothelium | Excitable cell |
|---|---|---|
| Selectivity | $K^+ > Rb^+ > Cs^+ > Li^+ > Na^+$ | $K^+ > Rb^+ > Cs^+ > Na^+ > Li^+$[a] |
| $\tau_{activate}$ | ≈ 4 msec | ≈1–23 msec[b,g] |
| | Voltage dependent | Voltage dependent[b] |
| $\tau_{inactivate}$ | 18 msec; 92 msec | 21–50 msec; 82–700 msec[b,e,h] |
| | Voltage independent | Voltage dependent[c], or independent[e,h] |
| $\tau_{reactive}$ | 156 msec | 20 msec–33 sec[c] |
| Activation threshold | −20 mV | −30 mV to −60 mV[b,f] |
| $V_{1/2\ activate}$ | 3.5 mV | −34 mV to −2 mV[g,h] |
| $k_{activate}$ | 15.0 mV | 5 mV[b] |
| $V_{1/2\ activate}$ | −41.98 mV | −3 mV to −110 mV[b,c] |
| $k_{inactivate}$ | − 9.1 mV | −15.8 mV to −6.8 mV[c,h] |
| 4-AP $K_d$ | 2.99 mM | 1.5 mM[d] |
| Quinidine $K_d$ | 10 μM | — |

[a] Taylor, 1987.
[b] Giles & Van Ginneken, 1985.
[c] Thorn et al., 1991.
[d] Thompson, 1977.
[e] Rogawski, 1988.
[f] Rogawski, 1985.
[g] Numann, Wadman & Wong, 1987.
[h] Oxford & Wagoner, 1989.

defined as the transient component. Figure 1*e* shows the instantaneous *I–V* relationship of the difference currents obtained using a tail current protocol in NaCl Ringer's solution (Fig. 1*d*). The current has been offset by the voltage required to bring the reversal potential ($E_{rev}$) in a $K^+$ Ringer's solution to 0 mV (−18.6 mV in this instance). The tail current pulse protocol (Fig. 1*d*, inset) consisted of holding the cells at a potential of −60 mV, stepping to a potential of +100 mV for a duration sufficient to achieve a maximum open probability ($P_o$) (usually 5–10 msec), and then generating tails using 8–10 pulses at +15 mV increments, starting at −80 mV. Figure 1(*c–e*) reveals a transient, outwardly rectifying current, with a reversal potential (−82 mV) close to that expected for a purely $K^+$-selective channel (calculated $E_{rev}$ = −87 mV). Similar transient currents were seen in 79 of 84 cells (94%) examined, with typical peak amplitudes between 70–200 pA.

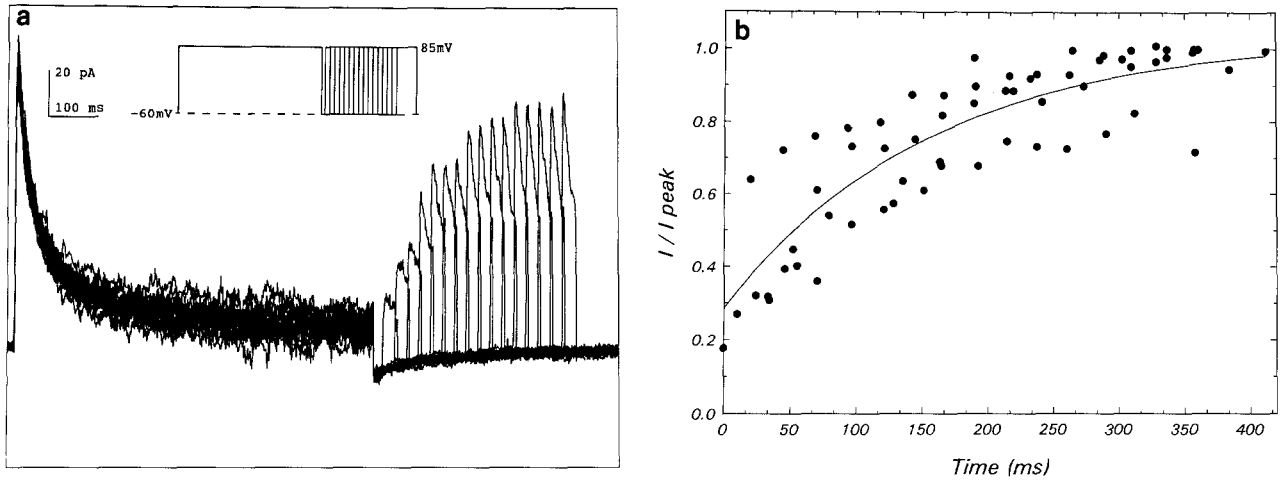


**Fig. 3.** (*a*) Recording of the difference current and pulse protocol for a single recovery from inactivation experiment. (*b*) Normalized current values from four experiments along with the curve generated by a single exponential fit to the data ($\tau_{reactivate}$ = 156 msec).

To further determine the transient channel's selectivity to monovalent ions, tail current experiments were performed using solutions 3–7 as the external solution. Instantaneous $E_{rev}$'s were obtained from the difference currents, and the bi-ionic potentials were calculated using

$$\left(\frac{P_A}{P_B}\right) = e^{E_{rev}ZF/RT} \cdot \left(\frac{B_i}{A_o}\right). \quad (1)$$

Where $P_A/P_B$ is the permeability ratio, $B_i$ is the concentration of intracellular ion, $A_o$ is the concentration or extracellular ion, and $RT/ZF$ has its usual meaning. This protocol reveals a selectivity for the channel of $K^+ > Rb^+ > Cs^+ > Li^+ > Na^+$, with permeability ratios equalling 1.00, 0.97, 0.10, 0.04, and 0.02, respectively ($n$ = 5) for each ratio determination.

The $I/I_{max}$ versus voltage relationship for the transient current is illustrated in Fig. 2. Steady-state inactivation of the current was determined by recording the peak values of the standard difference current at various holding potentials. Channel activation was determined using a modified tail current protocol. This protocol involved holding the cells at −60 mV, with activating pulses being applied in +10 mV steps from −80 mV up to +60 mV, followed by a hyperpolarizing pulse to −80 mV to generate the tails. Curves represent the fit to a Boltzmann distribution using the equation

$$I = I_{max}/(1 + e^{-(v-v_{1/2})/k}) + C \quad (2)$$

where $I_{max}$ = maximum peak current, $V$ = test voltage, $V_{1/2}$ = voltage at which $I = 0.5\ (I_{max})$, $k$ = slope factor, and $C$ = constant. Fit-determined parameters for both the activation and inactivation curves are listed in Table 2. All of these parameters are consistent with those for an *A*-type $K^+$ current. In addition, the fitted curves reveal a window current between −70 and −5 mV, which encompasses the resting voltage, with the maximum steady-state open probability occurring around −25 mV.

Figure 3*a* shows the difference currents from a single recovery from inactivation experiment along with the associated pulse protocol. This protocol consisted of holding the cell at −60 mV, applying a depolarizing pulse of +85 mV until the current had completely inactivated, then returning the cell to −60 mV for increasing time intervals followed by a +85 mV pulse, until the current again became fully activated. The cell in Fig. 3*a* shows complete inactivation of the A-current by the end of the 700 msec depolarizing pulse and complete reactivation by 350 msec. The normalized peak current versus time data from four inactivation recovery experiments is plotted in Fig. 3*b*, with currents normalized to the peak value of the initial current from each experiment. This data shows that the channel recovers from inactivation by approximately 300 msec. A single exponential fit to this data revealed a time constant for recovery from inactivation ($\tau_{reactivate}$) of 156 msec (Table 2).

To determine the voltage dependence of activation and inactivation, time constants of the difference currents obtained from tail and activation protocols were determined. Currents were fit using the Clampfit (Axon Instruments) software package. The voltage dependence of activation is clearly illustrated in Fig. 4*c*. In these experiments, the time

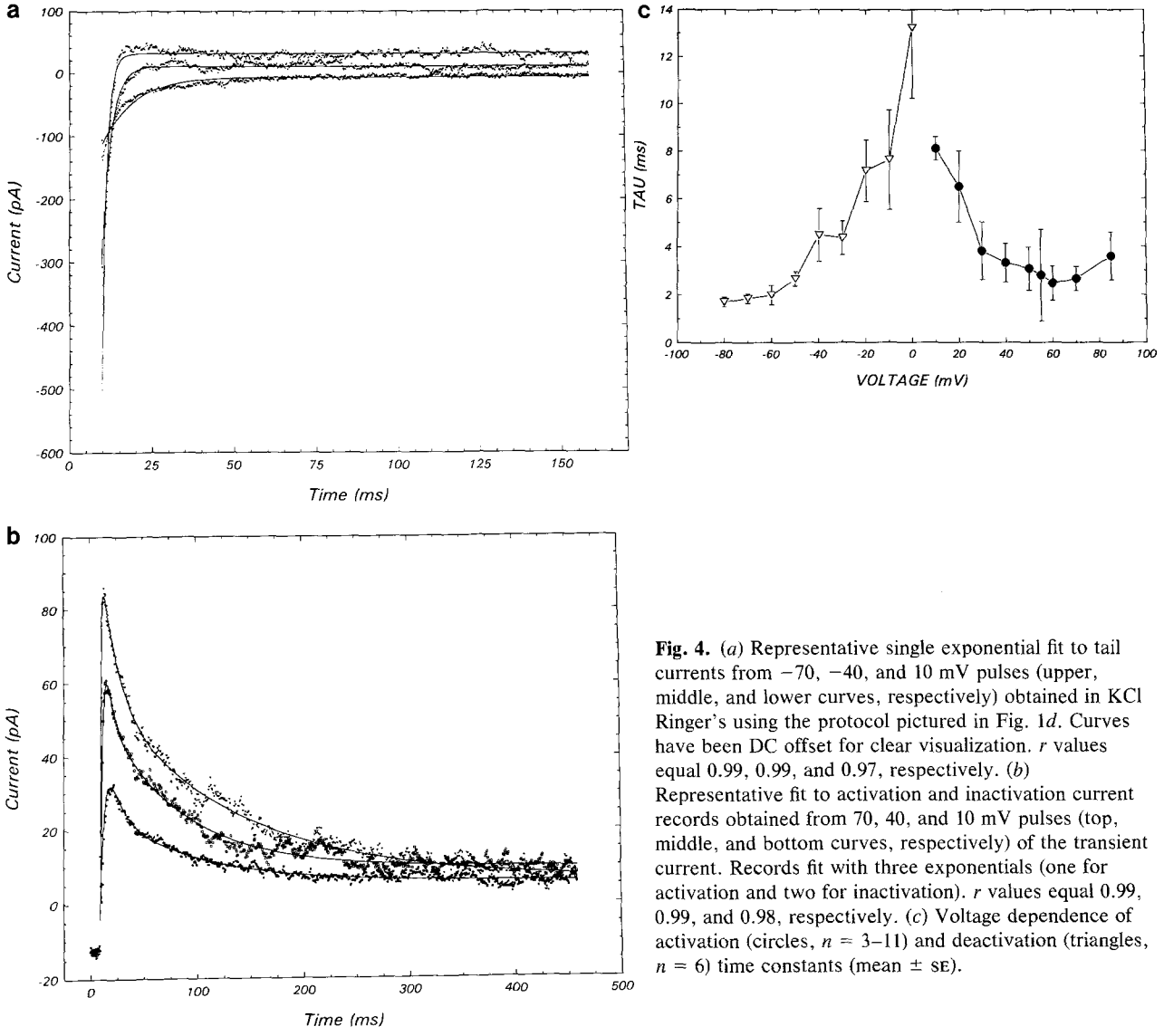


**Fig. 4.** (*a*) Representative single exponential fit to tail currents from −70, −40, and 10 mV pulses (upper, middle, and lower curves, respectively) obtained in KCl Ringer's using the protocol pictured in Fig. 1*d*. Curves have been DC offset for clear visualization. *r* values equal 0.99, 0.99, and 0.97, respectively. (*b*) Representative fit to activation and inactivation current records obtained from 70, 40, and 10 mV pulses (top, middle, and bottom curves, respectively) of the transient current. Records fit with three exponentials (one for activation and two for inactivation). *r* values equal 0.99, 0.99, and 0.98, respectively. (*c*) Voltage dependence of activation (circles, $n$ = 3–11) and deactivation (triangles, $n$ = 6) time constants (mean ± SE).

constants at hyperpolarized voltages were obtained by fitting the deactivation of tail currents (Fig. 4*a*), while those for depolarized voltages were obtained during the standard activation pulse protocol (Fig. 4*b*). Activation curves were fit by a single exponential, with $\tau$ between 2–14 msec. In several instances, deactivation curves were best fit using two exponentials. Because this was not a consistent scenario, we choose only to report the values for single exponential fits. Time constants for inactivation were also determined using the standard activation pulse protocol (Fig. 4*b*), and were best fit by two exponentials ($\tau$ = 18, 92 msec). Inactivation time constants were voltage independent (*data not shown*).

Block of the transient current by quinidine is illustrated in Fig. 5. Figure 5*a* shows the dose response of the *I–V* relationship for a single cell. It is apparent that 1 mM quinidine completely blocks the current. Figure 5*b* shows the peak current response versus quinidine concentration at +70 mV for the same cell as in Fig. 5*a*. Currents have been normalized to the peak of the control current. Fit of the data to the equation

$$y = 1/(1 + [X]/K_d) \quad (3)$$

where $K_d$ is the apparent dissociation constant and $[X]$ is the blocker concentration, yields a $K_d$ for quinidine of 0.01 mM at 50 mV. The fit is represented by the solid line through the data points in Fig. 5*b*. Partial block of the transient current was

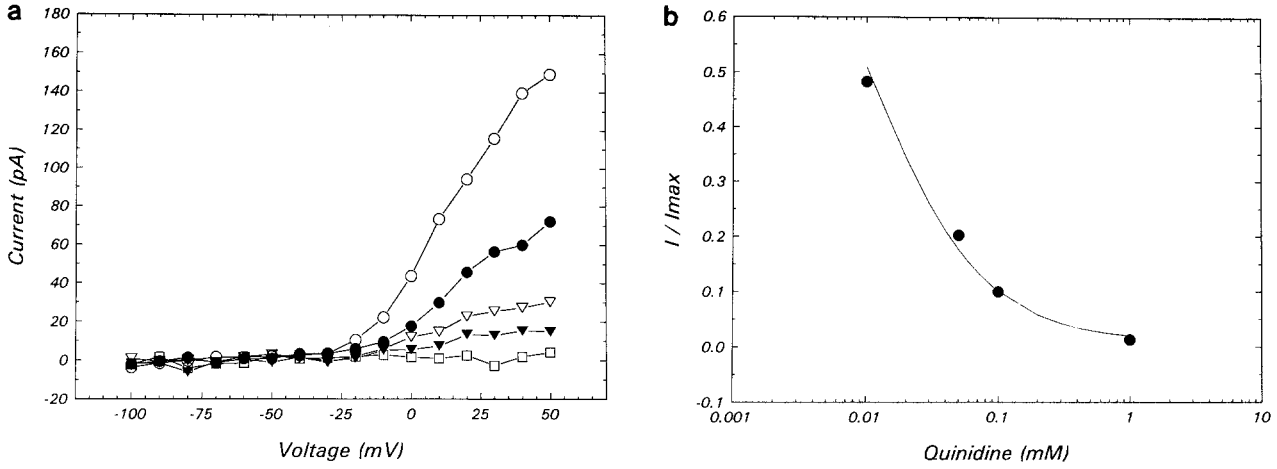


**Fig. 5.** (*a*) Peak current versus voltage curves (offset corrected) generated from standard difference currents for a cell exposed to several concentrations of quinidine in NaCl Ringer's: open circle = control; filled circle = 0.01 mM; open triangle = 0.05 mM; filled triangle = 0.1 mM; square = 1.0 mM. (*b*) Normalized peak current values versus quinidine concentration from *a*, along with fitted dose-response curve (*see* text for details). The calculated $K_d$ for quinidine at +50 mV = 0.01 mM.

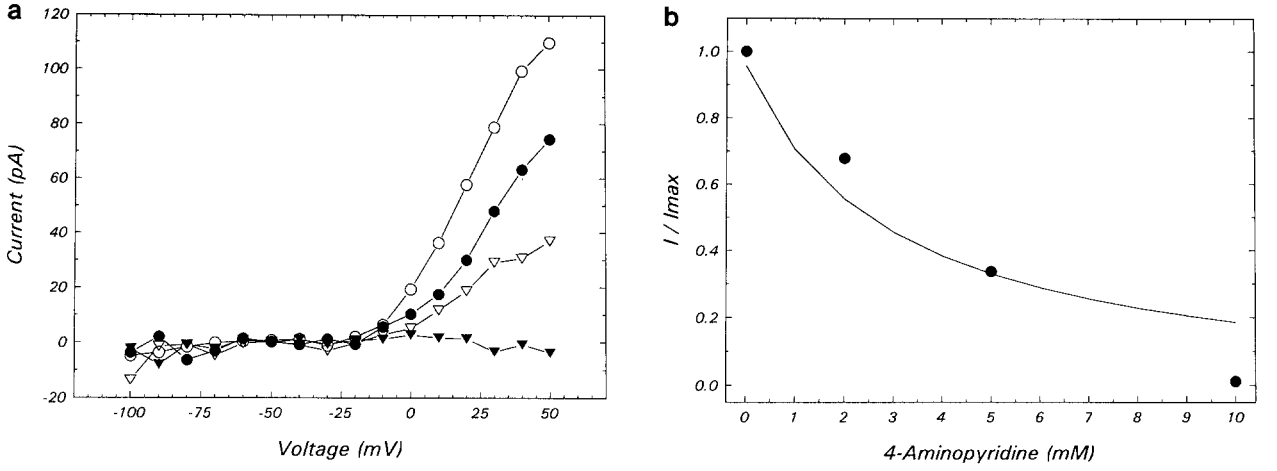


**Fig. 6.** (*a*) Peak current versus voltage curves (offset corrected) generated from standard difference currents for a cell exposed to several concentrations of 4-AP in NaCl Ringer's. Open circle = control; filled circle = 2.0 mM; open triangle = 5.0 mM; filled triangle = 10.0 mM. (*b*) Normalized peak current values versus 4-AP concentration from *a*, along with fitted dose-response curve (*see* text for details). The calculated $K_d$ for 4-AP = 2.99 mM.

seen immediately after application of quinidine, with 1–5 min being required for complete block. This block was only partially reversible.

Figure 6 illustrates the *I–V* relationship and dose response curve for a single cell treated with 4-aminopyridine (4-AP), a known blocker of transient $K^+$ currents. Figure 6*a* shows that 10 mM 4-AP is required to completely block the transient current. Fit of the normalized peak current versus 4-AP concentration data in Fig. 6*b* yields a $K_d$ for 4-AP of 2.99 mM at +50 mV. Block of the transient current by 4-AP occurred immediately and was only partially reversible. Neither tetraethylammonium (20 mM) nor barium (5 mM) blocked the transient current or its associated tail current (*data not shown*).

The residual currents remaining when holding the cells at 0 mV show a slight delay in activation and no signs of inactivation (Fig. 1*b*). The $E_{rev}$ of this current in $Na^+$ Ringer's solution is typically on the order of −15 mV (Fig. 7), when offset corrected by the same voltage required to bring the $E_{rev}$ in a $K^+$ Ringer's solution to 0 mV. This −15 mV $E_{rev}$ leads us to believe that the predominant current is a nonselective cation channel that shows either a small amount of selectivity for $K^+$ over $Na^+$, or has an extra component contributed by a small or sparse

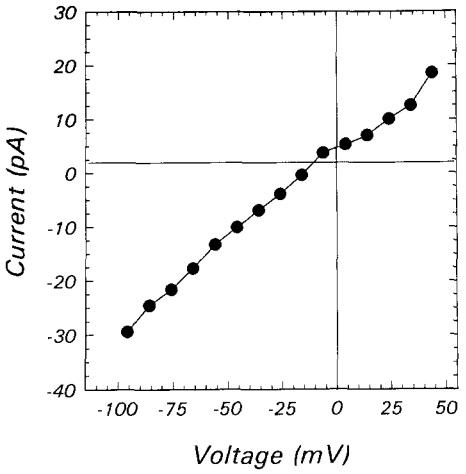


**Fig. 7.** Instantaneous *I–V* relationship generated from tail currents of a corneal endothelial cell held at a 0 mV resting potential in NaCl Ringer's solution.

$K^+$ channel. In traditional whole cell experiments using an internal solution containing 5 mM ATP (solution 2, Table 1), these currents are not blocked. Thus, the currents do not appear to be from the ATP-sensitive nonselective cation channel described previously in the endothelium by single channel analysis (Rae et al., 1991). The currents are blocked approximately 90% by inclusion of 1 mM quinidine in the bath.

### Perfusion Studies

Because quinidine blocks both the transient current and the residual currents seen at the 0 mV holding potential, as well as the nonselective cation channel described in single channel experiments, and a voltage-sensitive $Na^+$ channel described previously (Watsky et al., 1991), we choose to examine its effects on endothelial function using an in vitro perfusion system. This method equates endothelial pump function to changes in corneal thickness as measured by a specular microscope. Perfused corneas that show a negative or slightly positive swelling rate are assumed to have normal endothelial function, while those with a significantly positive swelling rate are deemed to be abnormal. The degree of swelling can be correlated to the state of disfunction of the endothelium. As seen in Fig. 8, addition of 1 mM quinidine to the perfusion solution caused a 48 $\mu$m/hr swelling rate, as compared to the 6 $\mu$m/hr swelling rate seen with the control GBR solution.

Once we determined that blocking the majority of the current types in the endothelium with quininidine created significant corneal swelling in the in vitro system, we proceeded to determine if the relatively selective blocker of the transient current, 4-AP, would also cause swelling. Figure 9 illustrates the results of the addition of 10 mM 4-AP to the perfusion media. Corneas perfused with 4-AP swelled at an average rate of 24 $\mu$m/hr, as compared to the deswelling rate of $-2$ $\mu$m/hr for control corneas perfused with GBR alone.

## Discussion

The corneal endothelium is a fluid transporting monolayer residing on the posterior surface of the corneal stroma. The cells of the endothelial monolayer are connected by "leaky" tight junctions. The imbibition pressure of the corneal stroma is such that aqueous humor is drawn across these tight junctions into the stroma, producing corneal swelling. It is the responsibility of the endothelium, primarily through $Na^+/K^+$ ATPase activity and its associated ion transporters and channels, to counteract this swelling tendency of the cornea. If the endothelium is compromised following disease or injury, the cornea becomes edematous and looses its transparency, resulting in blindness. Despite more than 30 years of research, the exact mechanisms of corneal endothelial transport have yet to be determined (Green, 1991).

The present study was designed to examine and characterize the whole-cell currents of the corneal endothelium and to determine if these currents play a role in the deturgescence mechanisms of this tissue. To date, the only whole-cell currents reported in the literature for corneal endothelium are from a voltage-sensitive, tetrodotoxin-blockable $Na^+$ channel (Watsky et al., 1991). As discussed in the Introduction, three other corneal endothelial channels have been described using single channel patch-clamp techniques. The predominant currents observed in the present study using the whole-cell technique do not seem to correspond to those described in the single-channel literature. Because all solutions used in the current study were $HCO_3$-free, we expected only minimal activation of the anion-activated $K^+$ channel observed previously in single-channel recordings (Rae et al., 1989). Because the open probability of this $K^+$ channel is increased to about 20% in the presence of $Cl^-$, it may be contributing some fraction to the residual whole cell current seen when holding the cell at 0 mV. Studies are currently under way to further characterize this fraction of the whole-cell current.

The A-type $K^+$ channel was originally described by Hagiwara, Kusano and Sato (1961) in molluscan neurons, and later characterized by Con-

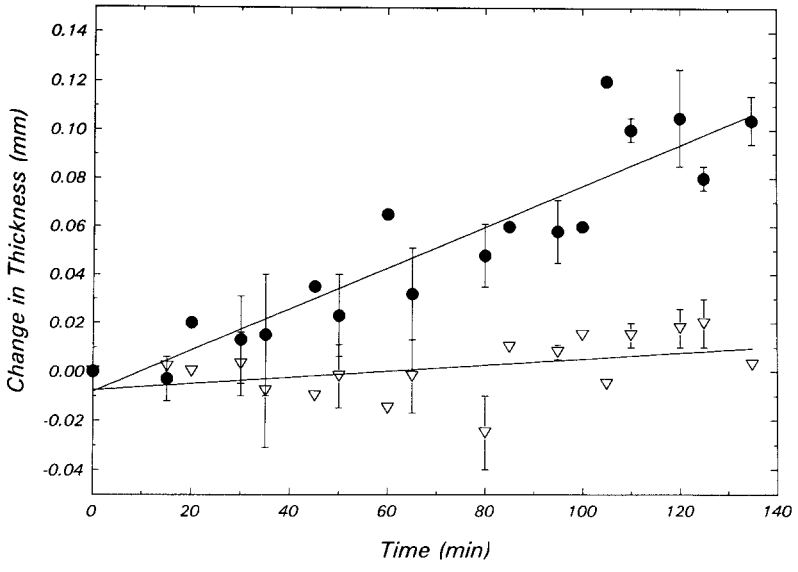


**Fig. 8.** Plot showing the change in thickness versus time for cells perfused with GBR and GBR + 1 mM quinidine ($n$ = 4; mean ± SE). Average starting thickness (at $t$ = 0) (± SE) for quinidine and control groups were 517 ± 4 μM and 504 ± 15 μM, respectively. Lines represent linear regressions through the data, whose slope was taken to be the swelling rate. Swelling rates for control and quinidine-perfused corneas equalled 6 and 48 μm/hr, respectively.

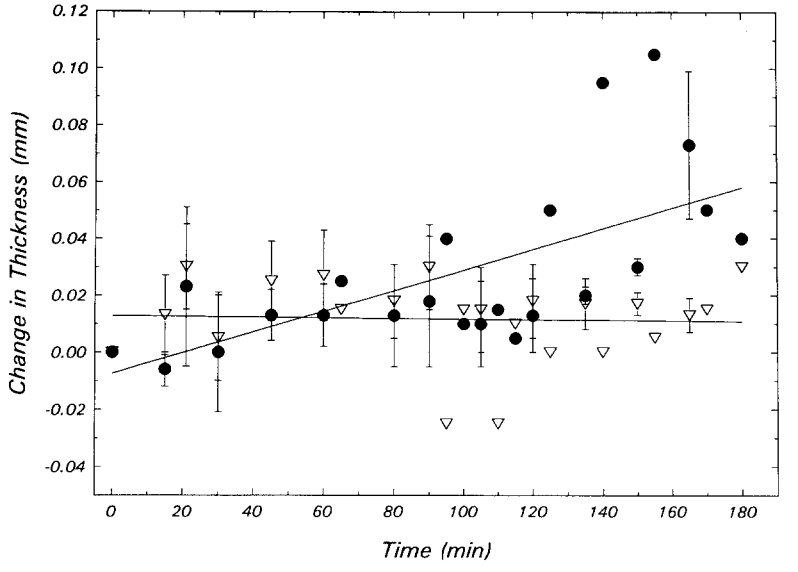


**Fig. 9.** Plot showing the change in thickness versus time for cells perfused with GBR and GBR + 10 mM 4-AP ($n$ = 6; mean ± SE). Average starting thickness (at $t$ = 0) (± SE) for 4-AP and control groups were 484 ± 11 μM and 486 ± 9 μM, respectively. Lines represent linear regressions through the data, whose slope was taken to be the swelling rate. Swelling rates from control and 4-AP perfused corneas equalled −2 and 24 μm/hr, respectively.

nor and Stevens (1971) and Neher (1971). It is a common feature of many excitable cells (Rogawski, 1985). The features of the transient current seen at hyperpolarized holding potentials in the corneal endothelium are very similar to those of the *A*-type currents. As seen in Table 2, almost all of the parameters examined in the corneal endothelium fall within the range of the corresponding parameters for some excitable cells. There is, of course, a wide range of values for corresponding parameters from different cell types reported in the literature (for a discussion *see* Thorn et al., 1991). This is the first report of an *A*-type current in any epithelial cell type.

The *A*-type current was observed in 94% of all cells examined and, in many, was the predominant whole-cell current at depolarized voltages. The corneal swelling observed in the 4-AP perfusion experiments (Fig. 9) tends to support the notion of a significant role for the *A*-type current in the deturgescence function of the endothelium. Interestingly, quinidine almost totally blocks the entire whole-cell current and elicits a swelling rate that is almost identical to that seen following corneal perfusion with $10^{-5}$ M ouabain (Geroski, Kies & Edelhauser, 1984). The normal resting potential of the endothelium at room temperature, the temperature at which this study was conducted, is around −39 mV (Watsky & Rae, 1991). Examination of Fig. 2 shows that this resting voltage is hyperpolar-

ized enough to keep channels responsible for the A-Type current from completely inactivating. On the other hand, channel activation would be limited due to the presumably stable nature of this resting voltage and the fact that it is not depolarized enough to substantially activate the current (Fig. 2). It is possible that the physiological role lies in the small open probability that exists in the window under the activation and inactivation curves. The highly active $Na^+/K^+$ ATPase of this tissue requires a $Na^+$ and $K^+$ recycling pathway to continue its normal function. The A-type current, which has a small but significant $P_o$ at rest, along with the channels blocked by quinidine, may provide this pathway. Assuming that corneal endothelial cells have a functional $Na^+/K^+$ ATPase pump site density similar to that of cardiac myocytes (approximately $1.2 \times 10^5$ sites/pF; Gadsby & Nakao, 1989), a turnover rate of approximately 100/sec (Harms & Wright, 1980; Gadsby & Nakao, 1989), and an average capacitance of 6.6 pF (*see* Results), the inward $K^+$ current produced by the $Na^+/K^+$ ATPase would be about 25 pA. Given an average peak A-type current of 135 pA and a peak window current $P_o = 0.13$ (Fig. 2), the peak window $K^+$ current would equal 18 pA. Thus the $K^+$ fluxes produced by the pump and the resting A-type current could balance accordingly. In addition, gating of the *A*-type channel may be influenced by factors other than voltage. This possibility is currently under investigation.

We would like to thank Dr. William Bourne for the use of his specular microscopy corneal perfusion apparatus and Helen Hendrickson for her technical assistance. This work was supported by NIH grants EY06206, EY03282, EY06005, and an unrestricted award from Research to Prevent Blindness.

## References

Connor, J.A., Stevens, C.F. 1971. Voltage-clamp studies of a transient outward membrane current in gastropod neural somata. *J. Physiol.* **213:**21–30

Dikstein, S., Maurice, D.M. 1972. The metabolic basis to the fluid pump in the cornea. *J. Physiol.* **221:**29–41

Gadsby, D.A., Nakao, M. 1989. Steady-state current-voltage relationship of the Na/K pump in guinea pig ventricular myocytes. *J. Gen. Physiol.* **94:**511–537

Geroski, D.H., Kies, J.C., Edelhauser, H.F. 1984. The effects of ouabain on endothelial function in human and rabbit corneas. *Current Eye Res.* **3:**331–338

Giles, W.R., Van Ginneken, A.C.G. 1985. A transient outward current in isolated cells from the crista terminalis of rabbit heart. *J. Physiol.* **368:** 243–264

Green, K. 1991. Corneal endothelial structure and function under normal and toxic conditions. *Cell. Biol. Rev.* **25:**169–207

Hagiwara, S., Kusano, K., Sato, N. 1961. Membrane changes in *Onchidium nerve cell in potassium-rich media. J. Physiol.* **155:**470–489

Harms, V., Wright, E.M. 1980. Some characteristics of Na/K-ATPase from rat intestinal basal lateral membranes. *J. Membrane Biol.* **53:**119–128

Neher, E. 1971. Two fast transient current components during voltage clamp on snail neurons. *J. Gen. Physiol.* **58:**36–53

Numann, R.E., Wadman, W.J., Wong, R.K.S. 1987. Outward currents of single hippocampal cells obtained from the adult guinea pig. *J. Physiol.* **393:**331–353

Oxford, G.S., Wagoner, P.K. 1989. The inactivating $K^+$ current in $GH_3$ pituitary cells and its modification by chemical reagents. *J. Physiol.* **410:**587–612

Rae, J.L., Cooper, K.E., Gates, P., Watsky, M.A. 1991. Low access perforated patch recordings using amphotericin B. *J. Neurosci. Methods* **37:**15–26

Rae, J.L., Dewey, J., Cooper, K. 1989. Properties of single potassium-selective ionic channels from the apical membrane of rabbit corneal endothelium. *Exp. Eye Res.* **49:**591–609

Rae, J.L., Dewey, J., Cooper, K., Gates, P. 1990. Potassium channel in rabbit corneal endothelium activated by external ions. *J. Membrane Biol.* **114:**29–36

Rae, J.L., Levis, R.A., Eisenberg, R.S. 1988. Ionic channels in ocular epithelia. *In:* Ion Channels. T. Narahashi, editor. pp. 283–327. Plenum, New York

Rogawski, M.A. 1985. The A-current: How ubiquitous a feature of excitable cells is it? *Trends Neurosci.* **8:**214–219

Rogawski, M.A. 1988. Transient outward current ($I_A$) in clonal anterior pituitary cells. Blockade by aminopyridine analogs. *Naunyn-Schmiedebergs Arch. Pharmacol.* **338:**125–132

Taylor, P.S. 1987. Selectivity and patch measurements of A-current channels in *Helix aspersa* neurones. *J. Physiol.* **388:**437–447

Thompson, S.H. 1977. Three pharmacologically distinct potassium channels in molluscan neurones. *J. Physiol.* **265:**465–488

Thorn, P.J., Wang, X., Lemos, J.R. 1991. A fast, transient $K^+$ current in neurohypophysial nerve terminals of the rat. *J. Physiol.* **432:**313–326

Watsky, M.A., Cooper, K., Rae, J.L. 1991. Sodium channels in ocular epithelia. *Pfluegers Arch.* **419:**454–459

Watsky, M.A., Rae, J.L. 1991. Resting voltage measurements of the rabbit corneal endothelium using patch-current clamp techniques. *Invest. Ophthalmol. Vis. Sci.* **36:**106–111

Received 22 July 1991; revised 28 January 1992